

SYNTHESIS AND CHARACTERIZATION OF CUBIC BaTiO₃ NANORODS VIA FACILE HYDROTHERMAL METHOD AND THEIR OPTICAL PROPERTIES

R.VIJAYALAKSHMI, V. RAJENDRAN*

Department of Physics, Presidency College, Chennai, TamilNadu, India

The single-crystalline perovskite barium titanate nanorods were successfully synthesized by a hydrothermal method. The synthesis was accomplished by using barium chloride and titanium tetrachloride as the starting materials and NaOH as mineralizer, respectively. The crystal structure, morphology and optical properties of the nanorods were characterized by XRD, SEM, TEM, UV and PL. The XRD results suggested that the hydrothermally synthesized BaTiO₃ nanorods are cubic phase. Well-isolated single-crystalline cubic perovskite BaTiO₃ nanorods with diameters ranging from 20 to 30 nm and lengths reaching up to >90 nm can be easily fabricated by this route. PL spectrum showed high UV emission and very low visible emission, indicating good quality of particles with little surface defects. The mechanism of the formation of the single-crystalline cubic perovskite BaTiO₃ nanorods was discussed.

(Received April 5, 2010; accepted May 19, 2010)

Keywords: BaTiO₃, Nanorod, Hydrothermal method, Synthesis, XRD, TEM, SEM, UV, PL

1. Introduction

Ceramic materials based on perovskite-like oxides are of significant interest because of their applications in electrical and electronic devices. The extensive application of barium titanate (BaTiO₃) in the ceramic industry is based on the properties of its polymorphs [1, 2]. The temperatures higher than about 130°C (Curie temperature), BaTiO₃ exists in the cubic perovskite structure. In this crystal structure, the Ba⁺² ions occupy the corners of the elementary cell, the Ti⁴⁺ ions are in the volume centre and the O²⁻ ions in the surface centre. Because of the high symmetry of the cubic phase, barium titanate exhibits paraelectricity and an isotropic dielectricity. Below the Curie point, the crystal structure transforms from the cubic phase to the distorted tetragonal structure with a displacement of the centers of positive and negative charges within the sublattice. As a result, a dipole moment parallel to one of the cubic axes of the original phase arises. Such a generated spontaneous polarization in the tetragonal structure is the origin of its ferroelectric and piezoelectric behaviour. Further reduction of the temperature changes the structure of BaTiO₃ into an orthorhombic structure at about 5°C and finally into the rhombohedral structure at 90°C. In fact, little study has been done for the latter two low-temperature modifications of BaTiO₃ and no industrial application of them has been reported [3, 4].

Cubic BaTiO₃ phase exhibits high dielectric constants [5]. As a dielectric material, BaTiO₃ is mainly used for capacitors such as multilayer ceramic capacitors (MLCCs) [6] and integral capacitors in printed circuit boards (PCB) [7]. Its polarization below Curie point can be applied for the use in dynamic random access memories (DRAM) [8]. Its piezoelectric properties enable its use in transducers and actuators [9]. Barium titanate nanorods have been synthesized by using different methods such as sol-gel processing [10], precipitation method [11], soft chemical process [12], sol-precipitation process [13], and a hydrothermal method [14]. Among them, hydrothermal method shows advantages as a simple system, low cost, without higher temperature calcinations

*Corresponding author: viji2302@gmail.com

process, controllable grain size and easy preparation for multi component sample etc. In this paper, we report the results on preparing nanorods of BaTiO₃ by the facile hydrothermal technique. The crystal structure, morphology and optical properties of BaTiO₃ nanorods are discussed for the first time via hydrothermal method.

2. Experimental procedure

Analytical grade barium chloride, titanium tetrachloride were adopted as the source material for barium and titanium, and sodium hydroxide as mineralizer. An aqueous solution of barium and titanium was obtained by mixing one molar stoichiometric of BaCl₂·2H₂O with 0.6mol of TiCl₄ in distilled water. A 1-3% concentration of NaOH was added to neutralize HCl formation from TiCl₄ hydrolysis and to keep the solution to a certain pH value. After adding NaOH the solution was stirred for 30 min, and resulting in a white colloidal sol, the final volume was adjusted to 90ml using deionized water. Thereafter, 90ml sol was transferred to a 100ml Teflon-lined auto clave vessel. The sealed vessel was heated to 240°C for 20 hrs. After that, the resultant precipitate was centrifuged and washed with water for several times and finally dried at 80°C for 12 hrs in a vacuum oven.

The as-prepared BaTiO₃ powder sample was characterized by X-ray powder diffraction on a D8 Advance X-ray diffractometer with CuK α irradiation at $\lambda=1.5406\text{\AA}$. The microstructure and grain size were analysed through a Scanning Electron Microscope Hitachi S-4500 and Transmission Electron Microscopy (TEM) using a JEM-2010 transmission electron microscope. The photoluminescence (PL) spectra were recorded at room temperature on a Hitachi model F-4500 fluorescence spectrophotometer. The optical absorption spectra were measured by a Cary 5E UV-Vis spectrophotometer (UV-2550).

3. Results and discussion

Fig. 1 shows a XRD pattern of hydrothermally as-synthesized barium titanate nanorods with different (1-3%) concentration of NaOH. It is shown that all patterns fit well with the peak positions of standard cubic-phase BaTiO₃. The inset Fig. 1 shows that only a single reflection is presented around a 2θ of 45°. Typically, the presence of the tetragonal form of barium titanate is inferred from the powder diffraction pattern containing two reflections due to (200) + (020) around a 2θ of 45°, whereas in the cubic form only a single reflection (200) is presented in this region. Therefore, the XRD pattern shown in Fig. 1 confirms that the BaTiO₃ are composed of cubic form of barium titanate. The peaks in the XRD pattern are strong and sharp, which indicate relatively high crystallinity of the powders. The existence of chlorine ion is a possible reason for the high crystallinity because chlorine ion has been proven to assist in the selective formation of crystalline oxides rather than amorphous oxides [15].

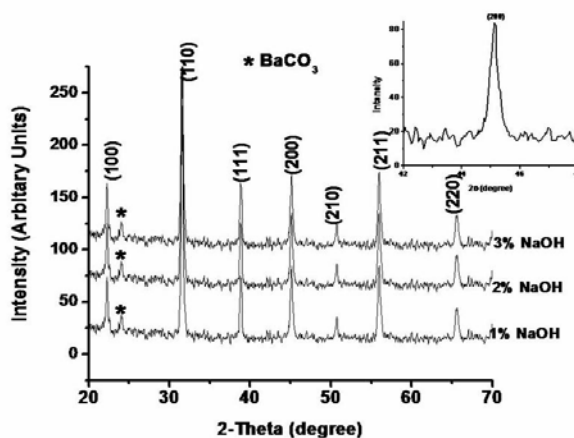


Fig. 1. Powder XRD of the BaTiO₃ powders with 1-3% concentration of NaOH. Inset shows that only a single reflection is present around a 2θ of 45°.

The crystallinity of BaTiO₃ (cubic) was estimated by measuring the XRD intensities of BaTiO₃ (cubic) (100) peak at $2\theta=22.160^\circ$ with few by-product of BaCO₃ (marked with asterisks) which can be removed by a washing process. The unit cell parameter for the crystalline BaTiO₃ is determined to be $a=3.994\text{\AA}$ and $c=4.035\text{\AA}$ which are consistent with the literature data of JCPDS (31-1741). The crystal size of BaTiO₃ was calculated to be = 25-30 nm from the broadening of the corresponding XRD peaks using the Scherrer equation: $L=K\lambda/(\beta\cos\theta)$, where L is the crystal size; λ is the wavelength of the X-ray radiation ($\lambda=0.15406\text{ nm}$) for Cu K α ; K is usually taken as 0.89; and β is the line width at half-maximum height.

SEM micrographs of BaTiO₃ powders synthesized at three different concentration of NaOH (1%, 2% & 3%) are shown in Fig.2 (a, b & c). Particle synthesized in 1% NaOH appear to be very uniform spherical morphology. In the case of 2% NaOH, particles were modified spherical into rod-like morphology. However, the BaTiO₃ particles synthesized in the 3% NaOH were completely changed into nanorods. With increasing the concentration of NaOH, the particles lose their acidity nature and then it converts amphoteric into basicity. By choosing the adequate concentration we could able to form nanorods.

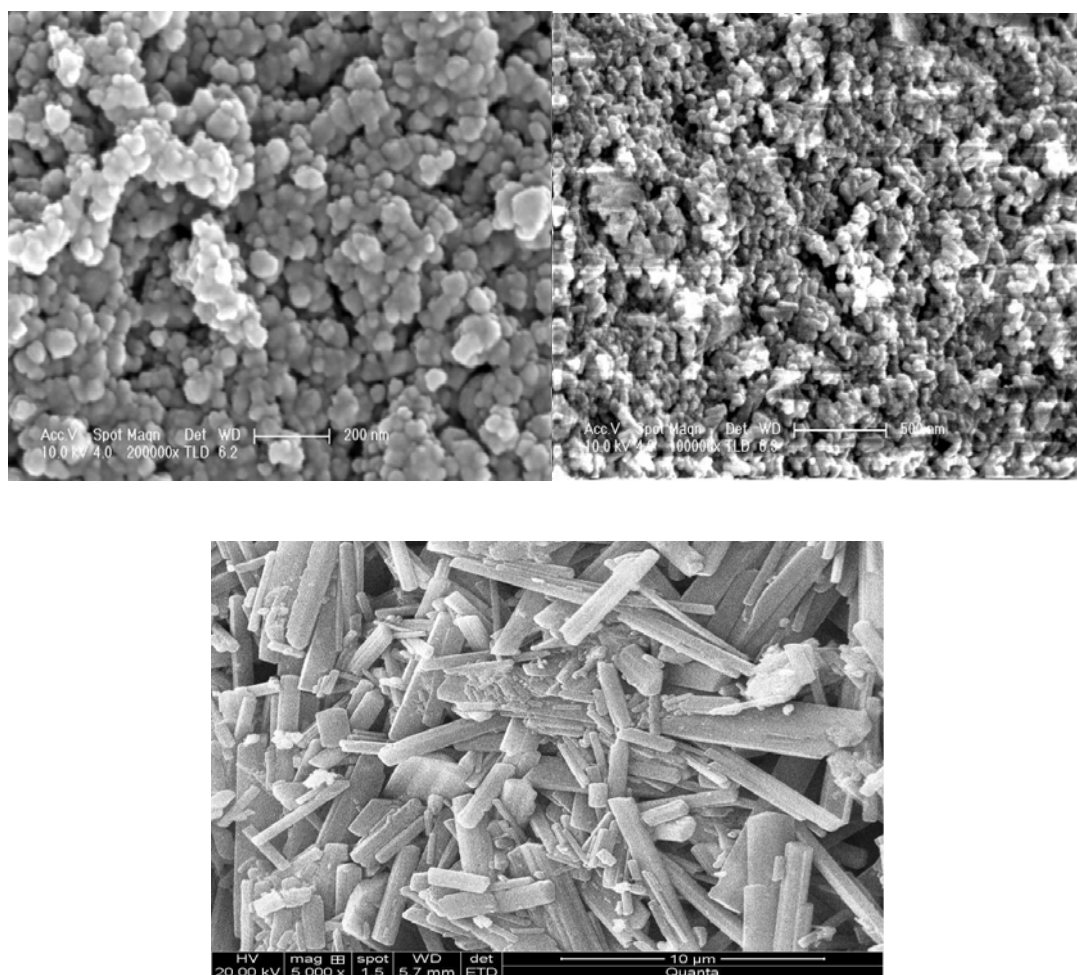


Fig.2 SEM image of the BaTiO₃ powders with different concentration of NaOH. 2(a) 1% NaOH, 2(b) 2% NaOH, 2(c) 3% NaOH.

Fig. 3(a) shows a TEM image of the barium titanate nanorods obtained by the addition of 3% NaOH. The BaTiO₃ nanorods are very straight and have a high regularity. TEM image shows that almost all of the nanoparticles in the reaction system were incorporated into the BaTiO₃ nanorods by oriented attachment mechanism. The diameter of the BaTiO₃ nanorods range from 20 to 30 nm and lengths reaching up to >90 nm. As shown in fig.3 (b) Selected Area Electron

Diffraction (SAED) pattern exhibits a sharp diffraction pattern consistent with the cubic structure, which demonstrated that all of the BaTiO_3 nanorods were single crystalline. The first four dots are assigned to the (100), (110), (111), and (200) reflections of the cubic phase and are in good agreement with the XRD measurements. Energy dispersive Spectrum (EDS) displayed in Fig.3(c) and inset table furnish the composition of various elements in the prepared sample.

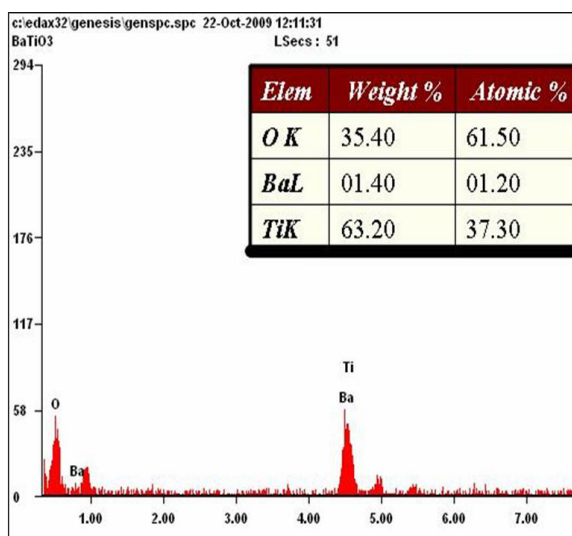
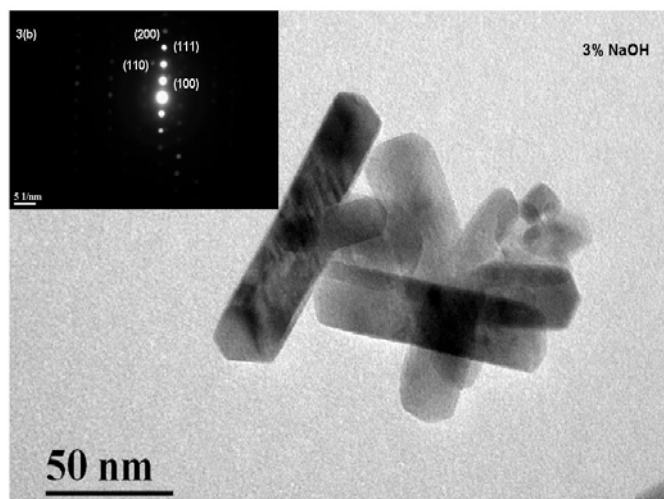


Fig. 3(a) TEM image of the BaTiO_3 powders with 1-3% concentration of NaOH. 3(b) Inset showed the SAED pattern of BaTiO_3 powders with 3% concentration of NaOH. 3(c) EDS of the BaTiO_3 powders with 3% concentration of NaOH.

Photoluminescence (PL) spectra of BaTiO_3 nanorods excited with a 350 nm laser source at room temperature are presented in Fig 4. PL spectra of BaTiO_3 nanorods consist of two bands: near band edge excitonic UV emission and defect related deep level emission in the visible range. The spectra display a strong UV bandgap emission around 369, 366 and 363 nm respectively. The emission in the UV region is attributed to the recombination between electrons in the conduction band and holes in the valence band. The visible emission is related to the intrinsic structural defects related to deep level emission, such as oxygen vacancies, surface states, OH^- defects and noncentral symmetric Ti^{3+} in the nanophase barium titanate. All these structural defects can give rise to a change in the octahedron configuration. A configuration co-ordinate model can be employed to elucidate the luminescence process in nanorods BaTiO_3 . In such a model, configuration coordinates can be used to describe the relative position of the ions inside the TiO_6

octahedron in perovskites BaTiO_3 . The electron band structure of BaTiO_3 has low-lying narrow conduction bands from Ti^{3+} -3d states and valence bands from O^{2-} -2p states [16]. Such a recombination corresponding to a charge transfer from the central Ti^{3+} ion to a neighboring O^{2-} ion inside the TiO_6^{8-} octahedron via intrinsic defects leads to luminescence in the nanorods BaTiO_3 system. Therefore a study of the PL property of BaTiO_3 can provide valuable information on the quality and purity of this material.

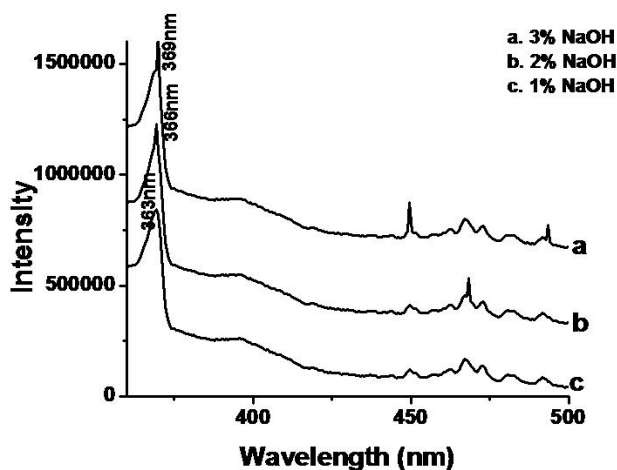


Fig. 4. Photoluminescence of BaTiO_3 powders for various concentrations (a) 3% NaOH (b) 2% NaOH (c) 1% NaOH.

The room temperature UV-Vis absorption spectrum of BaTiO_3 nanorods is shown in Fig. 5. The sharp rise of the spectra (1%, 2% & 3% NaOH) at the absorption edge demonstrates highly crystalline nanocrystals with less surface defects. The absorption band edges of the samples, showing obvious blue shift are estimated around 344, 329 & 315 nm. The values of bandgap energies in all three cases (3.6, 3.7 & 3.9 eV) are larger than that of the reported value for bulk BaTiO_3 (3.2 eV) which were also attributed to the formation of nanocrystalline BaTiO_3 particles [17]. Considering the blue shift of the absorption positions from the bulk BaTiO_3 , the absorption onsets of the present samples can be assigned to the direct transition of electron in the BaTiO_3 nanorods. Therefore, the BaTiO_3 nanorods would be a promising candidate for optoelectronic devices and UV Laser.

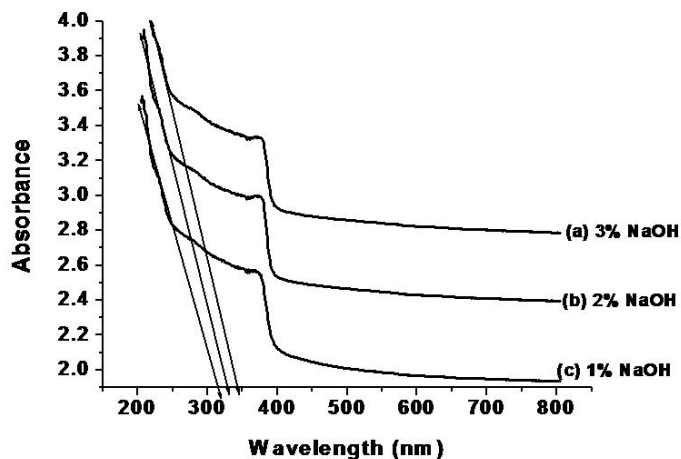


Fig. 5. UV-Vis Absorption spectrum of BaTiO_3 powders for various concentration (a) 3% NaOH (b) 2% NaOH (c) 1% NaOH.

The formation of cubic phase BaTiO₃ may be understood in the context of a dissolution-re-crystallization mechanism described by Eckert et.al. [18]. Compared other previous works used TiO₂ solid as titanium source; TiCl₄ could suppose more titanium ions for formation of BaTiO₃. At room temperature, when the sodium hydroxide was added in mixture solution of BaCl₂ and TiCl₄, the TiO₂ sol was formation. Increasing NaOH, the TiO₂ sol solubility also increases, thereby increasing the dissolution rate of titanium into solution and increasing the rate of BaTiO₃ formation.

From above results, it is proved that the importance of the hydroxide ions (OH⁻). They are not only vital in nucleation of BaTiO₃ crystals under hydrothermal conditions, from the standpoint of thermodynamics, as Leneka et.al. [19] reported, but they also seem to act as a catalyst by promoting the growth of BaTiO₃. Because sodium hydroxide solubility is more than barium hydroxide, in this work there are more OH⁻ ions in the solution than other previous works, then present work can prepared cubic BaTiO₃ by hydrothermal reaction only for 20 h. Two proposed mechanisms involve a condensation reaction of Ti(OH)₆²⁻ with Ba^{2+12b} and migration of Ba^{2+12a} into the TiO₂ structure with resulting breakage of Ti-O-Ti bands and incorporation of Ba²⁺. In the latter mechanism, the role of OH⁻ could be to facilitate the hydrolysis of Ti-O-Ti bands. The dynamic nature of the interaction between TiO₂, Ba²⁺, and OH⁻ leads to a crystallization mechanism involving nucleation, growth, and crystal dissolution.

The role of the Cl⁻ seems to be to help the nucleation of larger crystals with the smaller crystals acting as seed nuclei. It has been noted that in the presence of halide ions, the reactivity of TiO₂ is decreased. Even though the exact reason for this is unclear, it is possible that decreased reactivity could be due to absorption of the Cl⁻ on the TiO₂ surface, thus impeding the diffusion of Ba²⁺. If, as mentioned above, the cubic BaTiO₃ grows by a dissolution/re-crystallization process and Cl⁻ retards the crystal growth process, then it may be able to stabilize the formation of larger crystals [20]. This suggested role of Cl⁻ is speculative. However the data shown in this paper clearly suggest those additives that do not directly enter into the chemical reaction in the hydrothermal synthesis process can stabilize the formation of the cubic BaTiO₃ nanorods.

4. Conclusions

We have successfully synthesized nanorods BaTiO₃ by using the hydrothermal method. XRD results show that the nanorods are cubic phase. Well-isolated single-crystalline cubic form BaTiO₃ nanorods with diameters ranging from 20 to 30 nm and lengths reaching up to >90 nm can be easily fabricated by this route. PL spectrum showed high UV emission and very low visible emission, indicating good quality of particles with little surface defects. Blue shifts occurred in all the cases (344,329 & 315 nm) from that of bulk (390 nm), but a prominent shift was observed for 3% NaOH. Increasing the NaOH concentration was benefit for preparation of BaTiO₃ nanorods. The barium titanate nanorods would be a promising candidate for optoelectronic devices and UV laser.

Acknowledgment

The authors are grateful to the University Grant Commission, for extending financial assistance to carry out this work.

Reference

- [1] P. Gherardi, E.Matijevif, Colloid Surfact., **32**,257 (1988).
- [2] J.A.Kerchner, J.Moon, R.E.Chodelka, A.A.Morrone, J.H.Adair, ACS Symp. Ser., **681**, 106 (1998).
- [3] P.Nanni, M.Leoni, V.Buscaglia and G.Aliprandi, J.Eur.Ceram.Soc., **14**, 85 (1994).
- [4] L.K.Templeton and J.A.Pask, J.Am.Ceram.Soc. **42**(5), 212 (1959).
- [5] P.K.Dutta, R.Asiaie, S.A.Akbar and W.Zhu, Chem: Mater. **6**, 1542 (1994).

- [6] K.Kumar, Ceramic Capacitors: an overview, *Electron. Inf.Plann.* **25** (11), 559 (1998).
- [7] A.Rae, M.Chu and V.Ganinie, , *American Ceramic Society* **100**, 1 (1999).
- [8] J.Cott. Status report on ferroelectric memory materials, *Integr. Ferroelectr.* **20**(1-4), 15 (1998).
- [9] C.Buchal and M.Siegert, *Integr. Ferroelectr.* **35** (1-4), 1731 (2001).
- [10] R.Kavian and A.Saidi, *Journal of Alloys and Compounds*, **468**, 528 (2009).
- [11] J-F.Chen, Z-G.Shen, F-T.Liu, X-L.Liu and J.Yun, *Scripta Materialia*, **49**, 509 (2003).
- [12] S.Ghosh, S.Dasgupa, A.Sen and H-S.Maiti, **61**, 538 (2007).
- [13] K-M.Hung, W-D.Yang and C-C.Huang, **23**, 1901 (2003).
- [14] T.Yan, X-L.Liu, N-R.Wang and J-F.Chen, *Journal of crystal growth*, **281**, 669 (2005).
- [15] M.Henry, J.P.Olivet, J.Livage, in: D.R.Uhlmann and D.R.Ulrich, *Ultrastructure Processing of Advanced Materials*, John Wily and Son, Newyork (1992).
- [16] M.S.Zhang, Z.Yin, Q.Chen, W.Zhang and W.Chen, *Solid state communications*, **119**, 659 (2001).
- [17] M.Mori, T.Kineri, K.Kadono, T.Sakaguchi, M.Miya and H.Wakabayashi, *J.Am.Ceram.Soc.*, **78**(9), 2391 (1995).
- [18] J.O.Jr. Eckert, C.C.H-Houston, B.L.Gersten, M.M. Lencka and R.E. Riman, *J.Am.Ceram.Soc.* **79**(11), 2929 (1996).
- [19] M.M.Lencka and E.Riman, *Chem.Mater.*, **5**, 61 (1993).
- [20] K.Kajiyoshi, N.Ishizawa and M.Yoshimura, *J.Am.Ceram.Soc.*, **74**(2), 369 (1991).